Super-resolving single nitrogen vacancy centers within single nanodiamonds using a localization microscope

Min Gu, [*] **Yaoyu Cao, Stefania Castelletto, Betty Kouskousis, Xiangping Li**

Center for Micro-Photonics, Faculty of Engineering and Industrial Sciences, Swinburne University of Technology, Hawthorn VIC 3122, Australia
[*] *mgu@swin.edu.au*

Abstract: In this paper, we show super-resolving single nitrogen vacancy (NV) centers with a sub-20 nanometer resolution in a wide-field localization microscope based on the discovery of photoluminescence blinking in high-pressure high-temperature nanodiamonds (NDs). The photon statistics reveals that NDs containing not only single but also multiple NV centers show photoluminescence blinking. The combination of an atomic force microscope and an optical localization microscope built on the blinking feature enables the optically resolved two NV centers within single NDs for the first time. Our method establishes new avenues for studying nanoscale photon dynamics associated with single NV centers within NDs together with ND-based ultra-sensitive bioimaging devices.

OCIS codes: (100.6640) Superresolution; (180.2520) Fluorescence microscopy; (160.2540) Fluorescent and luminescent materials; (160.4236) Nanomaterials.

References and links

1. J. R. Maze, P. L. Stanwix, J. S. Hodges, S. Hong, J. M. Taylor, P. Cappellaro, L. Jiang, M. V. G. Dutt, E. Togan, A. S. Zibrov, A. Yacoby, R. L. Walsworth, and M. D. Lukin, "Nanoscale magnetic sensing with an individual electronic spin in diamond," Nature **455**(7213), 644–647 (2008).
2. N. M. Nusran, M. U. Momeen, and M. V. G. Dutt, "High-dynamic-range magnetometry with a single electronic spin in diamond," Nat. Nanotechnol. **7**(2), 109–113 (2011).
3. Y. R. Chang, H. Y. Lee, K. Chen, C. C. Chang, D. S. Tsai, C. C. Fu, T. S. Lim, Y. K. Tzeng, C. Y. Fang, C. C. Han, H. C. Chang, and W. Fann, "Mass production and dynamic imaging of fluorescent nanodiamonds," Nat. Nanotechnol. **3**(5), 284–288 (2008).
4. L. P. McGuinness, Y. Yan, A. Stacey, D. A. Simpson, L. T. Hall, D. Maclaurin, S. Prawer, P. Mulvaney, J. Wrachtrup, F. Caruso, R. E. Scholten, and L. C. L. Hollenberg, "Quantum measurement and orientation tracking of fluorescent nanodiamonds inside living cells," Nat. Nanotechnol. **6**(6), 358–363 (2011).
5. G. Balasubramanian, I. Y. Chan, R. Kolesov, M. Al-Hmoud, J. Tisler, C. Shin, C. Kim, A. Wojcik, P. R. Hemmer, A. Krueger, T. Hanke, A. Leitenstorfer, R. Bratschitsch, F. Jelezko, and J. Wrachtrup, "Nanoscale imaging magnetometry with diamond spins under ambient conditions," Nature **455**(7213), 648–651 (2008).
6. E. Rittweger, K. Y. Han, S. E. Irvine, C. Eggeling, and S. W. Hell, "STED microscopy reveals crystal colour centres with nanometric resolution," Nat. Photonics **3**(3), 144–147 (2009).
7. Y. K. Tzeng, O. Faklaris, B. M. Chang, Y. Kuo, J. H. Hsu, and H. C. Chang, "Superresolution imaging of albumin-conjugated fluorescent nanodiamonds in cells by stimulated emission depletion," Angew. Chem. Int. Ed. Engl. **50**(10), 2262–2265 (2011).
8. K. Y. Han, K. I. Willig, E. Rittweger, F. Jelezko, C. Eggeling, and S. W. Hell, "Three-dimensional stimulated emission depletion microscopy of nitrogen-vacancy centers in diamond using continuous-wave light," Nano Lett. **9**(9), 3323–3329 (2009).
9. J.-J. Greffet, J.-P. Hugonin, M. Besbes, N. D. Lai, F. Treussart, and J.-F. Roch, "Diamond particles as nanoantennas for nitrogen-vacancy color centers," arXiv:1107.0502v1 (2011).
10. E. Betzig, G. H. Patterson, R. Sougrat, O. W. Lindwasser, S. Olenych, J. S. Bonifacino, M. W. Davidson, J. Lippincott-Schwartz, and H. F. Hess, "Imaging intracellular fluorescent proteins at nanometer resolution," Science **313**(5793), 1642–1645 (2006).
11. M. J. Rust, M. Bates, and X. Zhuang, "Sub-diffraction-limit imaging by stochastic optical reconstruction microscopy (STORM)," Nat. Methods **3**(10), 793–796 (2006).
12. K. A. Lidke, B. Rieger, T. M. Jovin, and R. Heintzmann, "Superresolution by localization of quantum dots using blinking statistics," Opt. Express **13**(18), 7052–7062 (2005).

13. T. Dertinger, R. Colyer, G. Iyer, S. Weiss, and J. Enderlein, "Fast, background-free, 3D super-resolution optical fluctuation imaging (SOFI)," Proc. Natl. Acad. Sci. U.S.A. **106**(52), 22287–22292 (2009).
14. E. H. Chen, O. Gaathon, M. E. Trusheim, and D. Englund, "Wide-Field Multispectral Super-Resolution Imaging Using Spin-Dependent Fluorescence in Nanodiamonds," Nano Lett. **13**(5), 2073–2077 (2013).
15. B. Kouskousis, X. Li, S. Castelletto, and M. Gu, "Nanoscopic localisation and characterisation of nanoparticle embedded photonic materials," in *Quantum Electronics Conference & Lasers and Electro-Optics* (Melbourne, 2011), pp. 219–220.
16. C. Bradac, T. Gaebel, C. I. Pakes, J. M. Say, A. V. Zvyagin, and J. R. Rabeau, "Effect of the nanodiamond host on a nitrogen-vacancy color-centre emission state," Small **9**(1), 132–139 (2013).
17. C. Bradac, T. Gaebel, N. Naidoo, M. J. Sellars, J. Twamley, L. J. Brown, A. S. Barnard, T. Plakhotnik, A. V. Zvyagin, and J. R. Rabeau, "Observation and control of blinking nitrogen-vacancy centres in discrete nanodiamonds," Nat. Nanotechnol. **5**(5), 345–349 (2010).
18. M. Kuno, D. P. Fromm, S. T. Johnson, A. Gallagher, and D. J. Nesbitt, "Modeling distributed kinetics in isolated semiconductor quantum dots," Phys. Rev. B Condens. Matter **67**(12), 125304 (2003).
19. M. Kuno, D. P. Fromm, H. F. Hamann, A. Gallagher, and D. J. Nesbitt, ""On"/"off" fluorescence intermittency of single semiconductor quantum dots," J. Chem. Phys. **115**(2), 1028–1040 (2001).
20. K. T. Shimizu, R. G. Neuhauser, C. A. Leatherdale, S. A. Empedocles, W. K. Woo, and M. G. Bawendi, "Blinking statistics in single semiconductor nanocrystal quantum dots," Phys. Rev. B Condens. Matter **63**(20), 205316 (2001).
21. R. Verberk, A. M. Van Oijen, and M. Orrit, "Simple model for the power-law blinking of single semiconductor nanocrystals," Phys. Rev. B Condens. Matter **66**(23), 233202 (2002).
22. P. Siyushev, H. Pinto, A. Gali, F. Jelezko, and J. Wrachtrup, "Low Temperature Studies of Charge Dynamics of Nitrogen-Vacancy Defect in Diamond," arXiv:1204.4898v1 (2012).
23. G. Waldherr, J. Beck, M. Steiner, P. Neumann, A. Gali, T. H. Frauenheim, F. Jelezko, and J. Wrachtrup, "Dark states of single nitrogen-vacancy centers in diamond unraveled by single shot NMR," Phys. Rev. Lett. **106**(15), 157601 (2011).
24. B. Grotz, M. V. Hauf, M. Dankerl, B. Naydenov, S. Pezzagna, J. Meijer, F. Jelezko, J. Wrachtrup, M. Stutzmann, F. Reinhard, and J. A. Garrido, "Charge state manipulation of qubits in diamond," Nat Commun **3**, 729 (2012).
25. C. Kurtsiefer, S. Mayer, P. Zarda, and H. Weinfurter, "Stable solid-state source of single photons," Phys. Rev. Lett. **85**(2), 290–293 (2000).
26. T. Čižmár, M. Mazilu, and K. Dholakia, "In situ wavefront correction and its application to micromanipulation," Nat. Photonics **4**(6), 388–394 (2010).
27. B. P. Kouskousis, J. van Embden, D. Morrish, S. M. Russell, and M. Gu, "Super-resolution imaging and statistical analysis of CdSe/CdS Core/Shell semiconductor nanocrystals," J Biophotonics **3**(7), 437–445 (2010).
28. S. M. Mansfield and G. S. Kino, "Solid immersion microscope," Appl. Phys. Lett. **57**(24), 2615–2616 (1990).
29. S. A. Jones, S.-H. Shim, J. He, and X. Zhuang, "Fast, three-dimensional super-resolution imaging of live cells," Nat. Methods **8**(6), 499–505 (2011).

1. Introduction

Photoluminescent nitrogen vacancy (NV) centers in diamond, due to the possibility of coherent manipulation of their ground state electron spin, have considerable potentials for applications to engineered photonic systems such as nanoscale magnetic sensors and magnetic resonance imaging with single electron and nuclear spin sensitivity [1, 2]. NV centers in nanodiamonds (NDs) [3] offer a new bottom-up approach to develop nanophotonic systems [4, 5], however, the optical detection and control of nanometrically distributed single NV centers within NDs are limited by the diffraction barrier of far-field optics (~200 nm). Although the photostability of NV centers in bulk diamond has enabled the implementation of stimulated emission depletion (STED) microscopy with a resolution of 6 nm [6], the demonstrated resolution in NDs has never exceeded their sizes [7, 8], which is possibly attributed to the dielectric antenna effect [9]. Thus, multiple NV centers embedded in single NDs have never been optically resolved. Furthermore, the sequential scanning leads to slow frame rates, preventing live cell imaging and any dynamic process imaging to be conducted.

On the other hand, photoactivation localization microscopy (PALM) [10] and stochastic optical reconstruction microscopy (STORM) [11] enable the fast and super-resolved imaging/localization of single emitters, provided that their photoluminescence can be temporally switched on and off [12, 13]. Despite that the use of microwave probing has produced a mechanism for switching the photoluminescence enabling super-resolved imaging of NDs [14], this method with the intrinsic poor signal-noise-ratio (SNR) associated to the

optically detected spins has not allowed for the optical revolving of single NV centers within single NDs and further limited its wide-spread applications. Although the recent discovery of photoluminescence blinking of NV centers within NDs [15, 16] provides an alternative switching mechanism with sufficient SNRs, the blinking photon statistics associated with single NV centers within single NDs is yet to be determined prior to their application in a super-resolved localization microscope.

In this paper, we exploit the stochastic photoluminescence blinking of single NV centers within high-pressure high-temperature (HPHT) irradiated NDs using a localization microscope. The study of the photon statistics reveals that NDs containing not only single but also multiple NV centers show photoluminescence blinking. The stochastic photoluminescence on-off switching of NV centers and the associated non-bleaching property enable the reconstruction of a super-resolved image with sub-20 nm resolution. Consequently, optically resolved quantum dynamics of two or more NV centers within single NDs beyond their size limitation becomes possible for the first time.

2. Photon statistics of blinking NV centers

The scheme of super-resolving single NV centers within single NDs based on the photoluminescence blinking is illustrated in Fig. 1. The wide-field imaging of randomly distributed NDs emitting at different time sequences is illustrated in Figs. 1(a)-1(d). Analysis of images of NDs exhibiting stochastic photoluminescence blinking and subsequent determination of the centroids of emitters are used to reconstruct a nanometrically resolved image, as shown in Fig. 1(e).
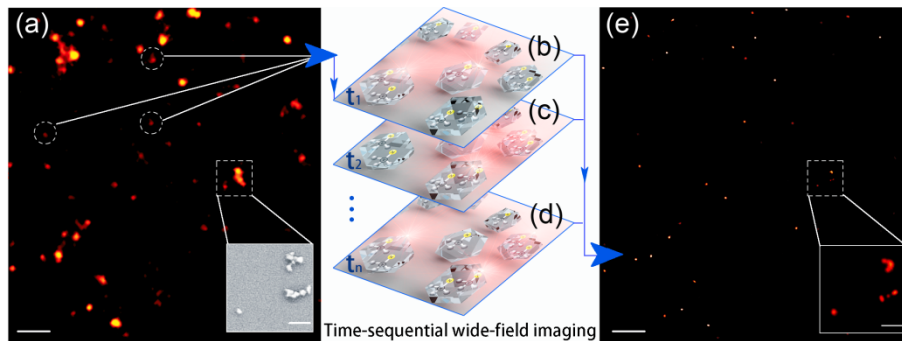

Fig. 1. Super-resolving single NV centers within HPHT NDs through a wide-field localization microscope. (a), A wide-field optical microscope image of HPHT NDs. The inset shows a scanning electron microscope (SEM) image of a typical sized HPHT ND indicated by the dashed square. (b-d), Schematic illustration of stochastic photoluminescence blinking images of nanometrically distributed HPHT NDs at three different time sequences. The blinking NDs indicated by the dashed circles are recorded at different time sequences and reconstructed by a home-made algorithm. (e), Super-resolution reconstructed image. The inset shows the zoomed-in view of the reconstructed image of the same area in the SEM image. The scale bars in (a) and (e) are 1 μm and those in insets are 200 nm.

The commercial HPHT 100 nm NDs containing multiple NV centers per ND [3], were centrifuged at the speed of 14,000 rpm for 10 minutes. Sonication procedures were also used to de-agglomerate the NDs in MilliQ solution. All the NDs were drop on oxygen asher plasma cleaned borosilicate cover slips and dried in air. The cover slips were marked using laser writing to characterize the same area of the sample with different methods such as wide-field localization microscopy, confocal microcopy and atomic force microscopy (AFM). Oxidation at 450°C for 2 h was used to further remove the residual graphitic layer on the surface of the NDs or other non-diamond material from the cover glass. Further oxidation at 600°C for 30 minutes was performed to reduce the size of the NDs after deposition and to increase the number of blinking diamonds. Initially, the percentage of photoluminescent NDs

that exhibited blinking in a wide-field image of 25 by 25 μm was typically less than 5%. However, after post-processing the size of the NDs reduced to approximately 75 nm or less, where the percentage of photoluminescent blinking NDs increased to over 40% [15]. It has been noticed that the observation of 10% NDs exhibiting blinking was recently reported through a similar approach [16].

To explore the photoluminescence blinking, we performed time-sequential wide-field imaging using a laser beam at the wavelength of 561 nm and an energy fluence of 140-530 KW/cm^2 for excitation. An oil immersion objective with numerical aperture (NA) of 1.4 and magnification of 100 times was used to excite and collect the photoluminescence from NDs. An ultra-steep edge long pass filter at the wavelength of 593 nm, and notch filters were used to stop the residual laser beam and select the emission of NV centers. Wide-field images at a duration of 30 ms were sequentially acquired using a cooled EMCCD camera (Andor, iXon X3 897) at − 80°C.
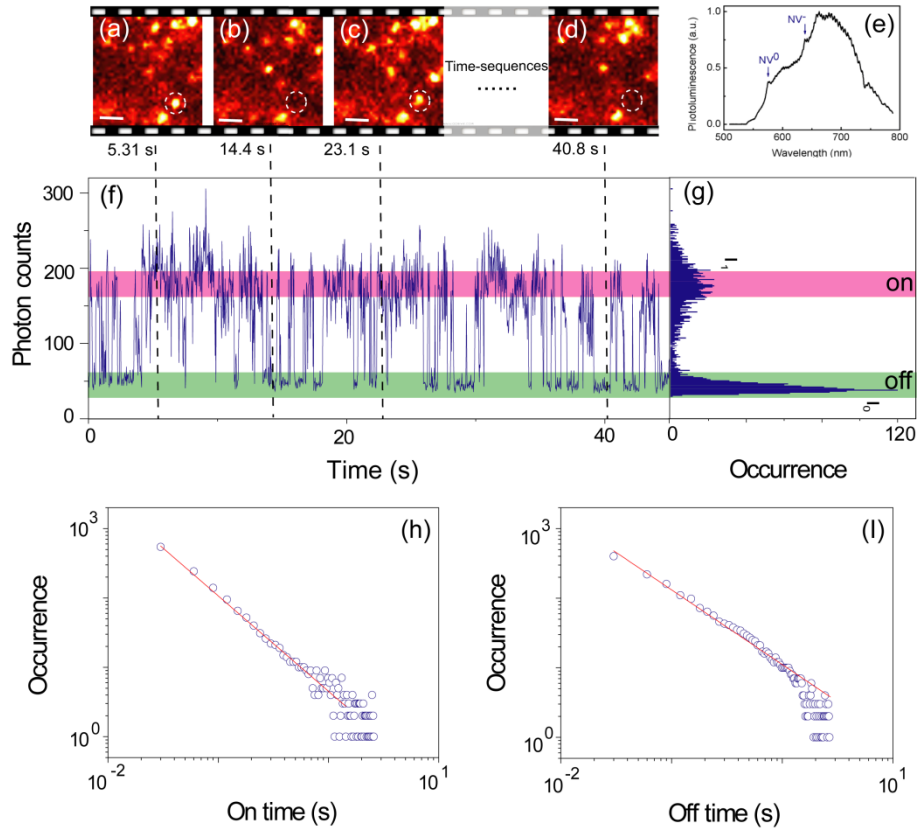

Fig. 2. Photoluminescence blinking behavior of HPHT NDs. (a)-(d), A typical stack of the time-sequential images of HPHT NDs showing photoluminescence blinking. (e), Emission spectrum of a blinking NV center within HPHT NDs as indicated by the dashed circle. Photoluminescence intensity trajectory (f) and histogram of intensity counts (g) of a blinking NV center within HPHT NDs. On-time $P(\tau_{on})$ (h) and off-time $P(\tau_{off})$ (i) probability of occurrence plots against the time durations.

A typical stack of the time-sequential photoluminescence images of post-processed NDs is displayed in Figs. 2(a)-2(d). The measured emission spectrum unambiguously confirms the origin of the observed photoluminescence blinking from NV centers within a ND, where the two charge stages, NV^0, with a zero-phonon line at the wavelength of 575 nm (2.156 eV) and

NV⁻, with a zero-phonon line at the wavelength of 637 nm (1.945 eV) can be distinctly identified in Fig. 2(e).

In order to retrieve on/off time durations, a histogram of photon counts per time bin was evaluated by using the photoluminescence trajectories of the blinking NDs. Analysis of these trajectories revealed that for the most part a simple two-state blinking behavior was observed, consistent with the previous observation of photoluminescence intermittence of NV centers in 5 nm sized detonation NDs [17]. For a comparison, the photoluminescence trajectories of detonation NDs were with less distinguishable on/off blinking contrast showing broad two-state distributions. In contrast, HPHT NDs exhibit two clearly separated distributions in Figs. 2(f) and 2(g), corresponding to the photoluminescence on and off states. The off-state was at the level of the background signal.
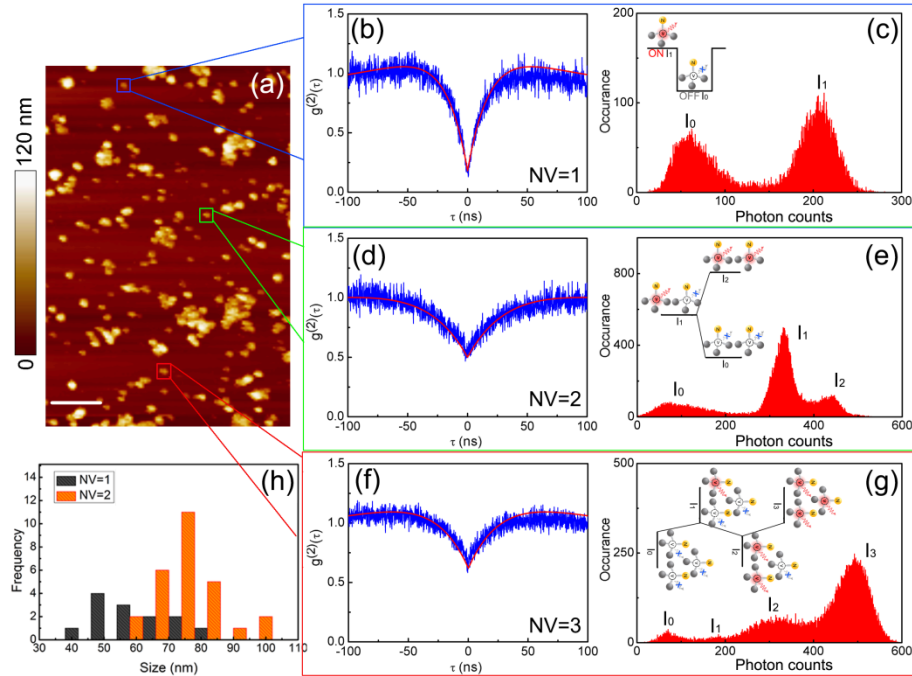

Fig. 3. Collective photoluminescence blinking of NV centers within single NDs. (a), AFM image of the photoluminescence blinking NDs. The scale bar is 1 μm. The color squares indicate the blinking NDs containing single (blue), two (green) and three (red) NV centers. Second-order correlation function $g^{(2)}(\tau)$ of single (b), two (d) and three (f) NV centers and corresponding histogram of photon counts showing two-state (c), three-state (e) and four-state (g) distributions, respectively. The insets schematically show the possible coupling states of multiple NV centers when located in the close proximity. (h) Statistic distribution of the size of single NDs containing 1 or 2 NVs.

By collecting all on/off time durations in a single trace, the corresponding probability of occurrence $P(\tau_{on/off})$ can be calculated as [18]

$$P(\tau_{on/off}) \approx \tau_{on/off}^{-m_{on/off}} \qquad (1)$$

Figures 2(h) and 2(i) display the on-time $P(\tau_{on})$ and off-time $P(\tau_{on})$ probability of occurrence plots against the time durations on a logarithmic scale, respectively. The linear fits with $m_{on} = 1.3$ and $m_{off} = 1.2$ reveal that the blinking behavior of NV centers follows a distinct power-law distribution. The values calculated here are comparable to those predicated by the typical power-law range of 1 to 2 for semiconductor quantum dots [19]. Therefore, it is

reasonable to point out that the power-law behavior in Eq. (1) indicates that the mechanism of photoluminescence blinking of NV centers may be ascribed to electron tunneling [18,20,21]. The spectral diffusion of NV centers in bulk and NDs which was recently ascribed to a photo-conversion process between a bright (very likely the negative charge state) and a dark (very likely the neutral charge state) state [22, 23], is less likely to be the only mechanism of the observed photoluminescence blinking. A possible dark state out of the spectral window of NV$^-$, associated to the yet unobserved NV$^+$, could be a cause of this blinking behavior [24]. Another effect, which most likely occurs in NDs, could be a shift of the Fermi level with respect to the charge transition level of the center, corresponding to the energy level at which the NV center takes up or losses an electron. This can be induced by surface charges and/or surface termination that could be more evident once the NDs size reduces or other defects like nitrogen are in the close proximity of the NV centers.

The photon statistics reveals that NDs containing not only single but also multiple NV centers exhibit photoluminescence blinking. The photon statistics from single NDs exhibiting photoluminescence blinking was determined through AFM in conjunction with a home-built confocal microscope using the Hanbury Brown-Twiss (HBT) interferometer. The normalized second-order temporal correlation function $g^{(2)}(\tau)$ at the zero delay time gave an indication of the number of emitters in a particular nanocrystal [25]. Figure 3 shows the second-order correlation function $g^{(2)}(\tau)$ of single blinking NDs as well as their corresponding histograms of the photon counts indicating the combination states of the collective blinking. The photoluminescence blinking of NV centers originating from single NDs was confirmed in the AFM image indicated by the squares, as shown in Fig. 3(a). In Figs. 3(b) and 3(c), $g^{(2)}(0) < 0.5$ indicates a single NV center within the ND, where a clearly separated two-state distribution was observed. In Figs. 3(d) and 3(e), two NV centers were identified by $g^{(2)}(0) \approx 0.5$, where a three-state distribution can be seen from the histogram of photon counts representing the off-state (I0) and one (I1) or two (I2) NV centers in the photoluminescence on-state, as schematically illustrated in the inset. A more complicated four-state distribution corresponding to the off-state (I0) and one (I1) or two (I2) or three (I3) NV centers in the photoluminescence on-state can be seen from the ND containing three NV centers, where $g^{(2)}(0) \approx 0.7$ in Figs. 3(f) and 3(g). In addition, we correlated the photon statistics with the size of the blinking nanocrystals using the images acquired from the AFM. We confirmed that most of the blinking NDs containing 2 NVs ($g^{(2)}(0) \approx 0.5$) have an average size of 75 nm, as shown in Fig. 3(h). Smaller NDs with a typical size of 50 ± 5 nm containing single NV centers were also observed, although with a less frequent distribution.

For most of their blinking duration, single NV centers spend approximately 50% of their time duration in the on-state and the other 50% in the off-state or dark state, where a typical example is shown in Fig. 3(c). In the case where more than two NV centers are located in close proximity within single NDs, the photoluminescence blinking statistics reveal a gradually transition to the on-state, where the on-state probability dominates over the off-state, implying a possible coupling between adjacent NV centers upon excitation. The collective photoluminescence blinking dynamics of multiple NV centers located in the diffraction limited region, which are not accessible by existing super-resolution methods, can now be clearly unveiled by our localization microscope.

3. Super-resolving single NV centers within single NDs

The localization microscope built on the stochastic photoluminescence on/off contrast opens the possibility of super-resolving single NV centers within single NDs to circumvent the diffraction barrier. The centroids of blinking NV centers were recorded at different time sequences and reconstructed for a super-resolved image with the localization precision determined by the number of photons collected. Unlike the fluorescent dye molecules which

show bleaching up to several tens of photoactivation cycles, NV centers with robust photostability at the highest irradiance fluence in our experimental condition enables more than 100 blinking cycles without bleaching. With a sufficiently large number of photons collected, the background noise becomes negligible and the error of the localization (σ) of the centroids can be expressed as [26]

$$\sigma = \sqrt{(s^2 + a^2/12)/N} \tag{2}$$

where s is the standard deviation of the point-spread function, a is the pixel size in the image and N is the total number of photons collected. The localization microscopy based on the high quantum yield and non-bleaching properties of NV centers enables an unprecedentedly high precision up to an atomic level, as shown in Fig. 4(a). The system drift was corrected by using a home-developed algorithm [27], which led to the measured accuracy of 12 nm (Figs. 4(b) and 4(c)). The discrepancy between the theoretical prediction and the measured accuracy is most likely attributed to the imperfect correction of the stage drift and focus shift during the measurement.
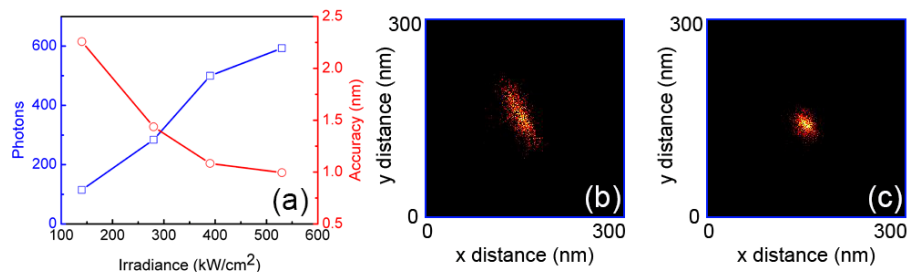

Fig. 4. (a) The localization accuracy as a function of the irradiance fluence. The blue squares represent the photons collected over a duration of 30 ms from a single NV center. The red circles represent the localization accuracy calculated using Eq. (2). The centroids of the fluorescence signals before (b) and after (c) system drift correction.
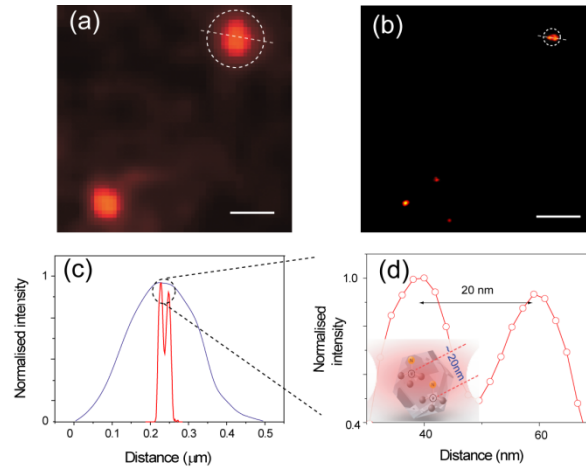

Fig. 5. Optically resolved single NV centers within a single ND. Comparison between wide-field image (a) and reconstructed super-resolution image (b) of NV centers within HPHT NDs. (c), The cross section plots of the same area in the wide-field image (purple) and super-resolution image (red) show that two NV centers with a separation of 20 nm can now be optically resolved. (d), The zoomed-in view of the cross section in the super-resolution image. The inset schematically illustrates two NV centers located within a single ND with a separation of 20 nm. The scale bar is 200 nm.

With an accuracy better than 12 nm in our approach, super-resolving single NV centers within single 75 nm sized NDs becomes possible for the first time. 2000 time-sequential images with a 30 ms duration for each image were analyzed to optically resolve two proximal NV centers within single NDs determined by the AFM image and the photon statistics. Figures 5(a) to 5(d) show the comparison of a wide-field image with the super-resolution reconstructed image. Indeed, our results can clearly resolve two NV centers embedded within a single ND with a separation of 20 nm for the first time.
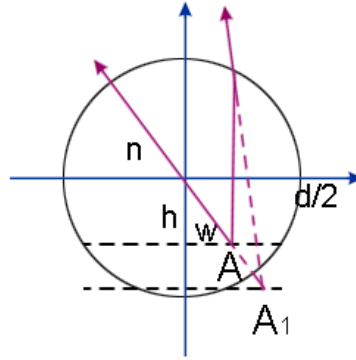

Fig. 6. Geometrical optical illustration of imaging a NV located at position A within the ND into a virtual image at position A_1 by a spherical shaped ND with a diameter of d.

As the high refractive-index dielectric environment in NDs may form a solid immersion lens and result in a virtual image of emitters, the observed 20 nm separation may not reflect the physical separation between the two NVs. The magnification of the virtual image is strongly dependent on the shape of the ND as well as the location of the NV. For the simplicity, Fig. 6 illustrates the formation of the virtual image of a NV located at a position (h, w) with respect to the center of a spherical shaped ND. Based on the approximation of geometrical optics, the magnification is approximately proportional to the square refractive-index of the lens [28]. The observed 20 nm separation indicates a possible physical separation of ~3.5 nm between the two NV centers.

4. Conclusion

We have shown super-resolving single NV centers within NDs with a sub-20 nanometer resolution in a wide-field localization microscope based on the photoluminescence blinking. The combination of an AFM and a localization microscope has enabled two NV centers embedded within single ND to be super-resolved for the first time. In addition, it reveals a collective blinking effect between NV centers located in nanometric distances. Our work opens a new avenue for studying intrinsic quantum interaction of single NV centers within single NDs associated with a nanoscale environment, which constitutes a viable method to further advance nanoscopy based on the blinking behavior of NV centers and holds enormous potentials in the application for super-resolution imaging in life sciences [29]. Finally, combining these results with the microwave excitation could provide an alternative image contrast for future magnetometry and biological imaging.

Acknowledgment